

Numerical study of hydrodynamics using the nonlinear Schrödinger equation

C. Nore^a, M.E. Brachet^a and S. Fauve^b

^aENS Ulm, Laboratoire de Physique Statistique, CNRS URA 1306, 24 rue Lhomond, 75231 Paris cedex 05, France

^bENS Lyon, Laboratoire de Physique, CNRS URA 1325, 46 Allée d'Italie, 69364 Lyon cedex 07, France

Received 29 July 1992

Accepted 18 November 1992

Communicated by A.C. Newell

The hydrodynamical behavior of the nonlinear Schrödinger equation is investigated by Fourier pseudo-spectral direct numerical simulations. Its dispersive and nonlinear acoustics are characterized quantitatively and an equation that describes this regime at leading order is derived. A technique that allows the preparation of periodic initial data containing an arbitrary system of point vortices with minimal acoustic excitations is given. The Eulerian dynamics of a jet made of an array of counter rotating vortices is obtained. Sinuous and varicose instabilities are shown to take place. Finally the numerical methods best suited to study vortex-sound interactions are discussed.

1. Introduction

The nonlinear Schrödinger equation (NLSE) governs the complex amplitude $A(\mathbf{r}, t)$ of quasi monochromatic wave trains in dispersive and nonlinear media [1]. It is also used to describe superfluid liquid helium II at zero temperature, as a semi-classical approximation for an assembly of bosons with local interactions [3]. The NLSE reads

$$\frac{\partial A}{\partial t} = i \Omega A + i \alpha \Delta A - i \beta |A|^2 A. \quad (1)$$

In the case of nonlinear media, α represents dispersion and β traces back to the frequency variation of the nonlinear wave with amplitude. We only consider here the “defocusing” case $\alpha\beta > 0$, in which monochromatic waves of constant amplitude are stable. In the case of superfluid helium, $A(\mathbf{r}, t)$ is the wave function of the Bose condensate and $\xi = \sqrt{\alpha/\Omega}$ is known as the “healing” length.

By scaling appropriately time, space and amplitude, we can set without loss of generality $\Omega = 1$, $\alpha = 1/2$ and $\beta = 1$.

The NLSE can be cast into a fluid dynamic form through the Madelung transformation [3,4]

$$A(\mathbf{r}, t) = R(\mathbf{r}, t) \exp[i\varphi(\mathbf{r}, t)]. \quad (2)$$

This change of variable in (1) gives

$$\frac{\partial R^2}{\partial t} + \nabla \cdot (R^2 \nabla \varphi) = 0, \quad (3)$$

$$\frac{\partial \varphi}{\partial t} + \frac{1}{2} (\nabla \varphi)^2 = 1 - R^2 + \frac{\Delta R}{2R}. \quad (4)$$

Eqs. (3) and (4) can be considered as the equations of conservation for mass and momentum of a compressible inviscid fluid of density $\rho(\mathbf{r}, t) = R^2$ and velocity $\mathbf{v}(\mathbf{r}, t) = \nabla \varphi$. Note that the Madelung transformation is singular when $R = 0$, i.e. when both the real and the imaginary parts of $A(\mathbf{r}, t)$ vanish. As two conditions are required, the singularities generically happen on

points in two dimensions and lines in three dimensions. The circulation of \mathbf{v} around such a generic singularity is 2π . These topological defects are known in the context of superfluidity as quantum vortices [3]. Away from the vortices, the vorticity $\Omega = \nabla \times \mathbf{v}$ is zero and eqs. (3) and (4) give

$$\frac{\partial \rho}{\partial t} + \nabla \cdot (\rho \mathbf{v}) = 0, \quad (5)$$

$$\frac{\partial \mathbf{v}}{\partial t} + (\mathbf{v} \cdot \nabla) \mathbf{v} = -\frac{1}{\rho} \nabla \left(\frac{\rho^2}{2} \right) + \nabla \left(\frac{\Delta \sqrt{\rho}}{2\sqrt{\rho}} \right). \quad (6)$$

The first term in the r.h.s. of eq. (6) corresponds to an equation of state with pressure $p = \rho^2/2$. The second term, called the “quantum mechanical pressure”, has no analog in standard fluid mechanics.

Our purpose is to show that NLSE can directly be used to study non trivial flows in inviscid fluid dynamics. This article is organized as follows: in section 2, we derive a nonlinear equation in the approximation of acoustics from NLSE and present some related numerical results. In section 3, we use NLSE to perform a numerical study of the instability of a double array of counter rotating vortices. We conclude by summarizing our results and discussing the different possible numerical methods for future studies of the delicate problem of sound-vortex interaction and sound emission by vortices.

2. The approximation of acoustics

We first consider small variations around a mean density $\rho_0 = 1$, and write

$$\rho = \rho_0 + \epsilon \rho_1 + \dots, \quad (7)$$

$$\mathbf{v} = \epsilon \mathbf{v}_1 + \dots. \quad (8)$$

We get to leading order from eqs. (5) and (6)

$$\frac{\partial^2 \rho_1}{\partial t^2} \approx \Delta \rho_1 - \frac{1}{4} \Delta^2 \rho_1, \quad (9)$$

showing that long wavelength perturbations propagate with a wave velocity 1. At wavelengths smaller than the healing length $\xi = 1/\sqrt{2}$, dispersive effects become important and thus modify the dynamics compared to usual gas dynamics. Note that they correspond to the quantum pressure term $\Delta \sqrt{\rho}/\sqrt{\rho}$.

To take into account nonlinear effects, it is simpler to work with the velocity potential φ . Using eq. (2) with $R = \sqrt{(1+2s)}$, we get from NLSE:

$$\frac{\partial \varphi}{\partial t} = -2s - \frac{1}{2} (\nabla \varphi)^2 + \frac{\Delta s}{2(1+2s)} - \frac{(\nabla s)^2}{2(1+2s)^2}, \quad (10)$$

$$\frac{\partial s}{\partial t} = -\nabla s \cdot \nabla \varphi - \frac{1}{2} (1+2s) \Delta \varphi. \quad (11)$$

The appropriate scaling for long-wavelength propagative disturbances,

$$\varphi = \mathcal{O}(1), \quad s = \mathcal{O}(\epsilon),$$

$$|\nabla| = \mathcal{O}(\epsilon), \quad \frac{\partial}{\partial t} = \mathcal{O}(\epsilon),$$

gives up to order ϵ^4 ,

$$\frac{\partial \varphi}{\partial t} \approx -2s - \frac{1}{2} (\nabla \varphi)^2 + \frac{1}{2} \Delta s, \quad (12)$$

$$\frac{\partial s}{\partial t} \approx -\frac{1}{2} \Delta \varphi - \nabla s \cdot \nabla \varphi - s \Delta \varphi. \quad (13)$$

The change of variable

$$s = u + \frac{1}{4} \Delta u$$

leads to

$$\frac{\partial \varphi}{\partial t} \approx -2u - \frac{1}{2} (\nabla \varphi)^2, \quad (14)$$

$$\frac{\partial u}{\partial t} \approx -\frac{1}{2} \Delta \varphi - \nabla(u + \frac{1}{4} \Delta u) \cdot \nabla \varphi - (u + \frac{1}{4} \Delta u) \Delta \varphi - \frac{1}{4} \Delta \frac{\partial u}{\partial t}. \quad (15)$$

which can be put under the form

$$\frac{\partial^2 \varphi}{\partial t^2} \approx \Delta \varphi - \frac{1}{4} \Delta^2 \varphi - \frac{\partial \varphi}{\partial t} \Delta \varphi - \frac{\partial (\nabla \varphi)^2}{\partial t} - \frac{1}{2} \nabla \cdot ((\nabla \varphi)^2 \nabla \varphi). \quad (16)$$

Note that the form of eq. (16) traces back to invariances of NLSE, space reflection symmetry, $\nabla \rightarrow -\nabla$, and time reversal symmetry which implies the invariance of (16) under the transformation, $t \rightarrow -t$, $\varphi \rightarrow -\varphi$. So, the quadratic nonlinearities of (16) should involve an even number of space derivatives and an odd number of time derivatives. The Galilean invariance of NLSE,

$$A(\mathbf{r}, t) \rightarrow A(\mathbf{r} - \mathbf{c}t, t) \exp[i(\mathbf{c} \cdot \mathbf{r} - \frac{1}{2} \mathbf{c}^2 t)], \quad (17)$$

is also preserved in (16).

Consequently, eq. (16) describes the nonlinear and dispersive dynamics of the phase to leading order, keeping the relevant invariances of NLSE. Note that for a one-dimensional field, and restricting to one direction of propagation, eq. (16) reduces to the Boussinesq equation for the phase-gradient. It is well known that for small amplitude perturbations, the phase-gradient of A in NLSE obeys the Boussinesq [1] or the Korteweg–de Vries [2] equations. However one has to select a direction of propagation and a particular Galilean reference frame to perform such a reduction. Therefore we consider that (16) is less restrictive to study the weakly nonlinear acoustics of NLSE.

In order to quantify the dispersive and nonlinear acoustic behavior of NLSE, we have performed numerical simulations in one space dimension using a standard Fourier pseudo-spectral method [5]. We chose a simple leap-frog time stepping for the nonlinear term and an exponential propagation for the linear term of the form

$$A(t + \Delta t) = e^{2L \Delta t} A(t - \Delta t) + \frac{e^{2L \Delta t} - 1}{L} f(t),$$

where f stands for the nonlinear term and L is

the linear operator in Fourier space. In order to suppress a possible odd–even instability, we do periodically a “mixing” step of the form

$$\tilde{A}(t) = \frac{1}{4} [A(t - \Delta t) + 2A(t) + A(t + \Delta t)].$$

This scheme is symmetrical under time reversal and globally second order in time. The code was validated by comparison with analytical soliton solutions of NLSE. We have found that 256 Fourier modes are enough to properly resolve these solutions.

We have studied the acoustic behavior by using initial data of the form

$$A(x) = 1 + a e^{-x^2/l^2}.$$

The results are shown in figs. 1, 2 and 3 for various values of a and l . Fig. 1 displays the linear dispersionless regime, where the initial disturbance gives rise to two counter-propagating pulses at velocity 1. Dispersive effects due to the “quantum mechanical pressure” are clearly noticeable in fig. 2. The Fourier components of the initial disturbance propagate at different velocities and this generates the wave-packet that travels ahead of the pulses, roughly at the group velocity, $\|\mathbf{v}_g\| = \partial(\sqrt{k^2 + k^4/4})/\partial k$. We measure $\|\mathbf{v}_g\| = 2.32$, that agrees within 3% with the predicted value for $k = \pi/\sqrt{2}$. The nonlinear effect present in fig. 3 can be distinguished from the linear dispersive effect of fig. 2 by the scale of the generated wavetrains. In the nonlinear case, the scale of the wavetrain is much smaller than the scale of the initial perturbation. The pulses travel faster than in the linear regime, which traces back to the linear velocity renormalization by the nonlinear terms. We have to leading order from (16) for a pulse of amplitude u propagating to the right

$$\frac{\partial^2 \varphi}{\partial t^2} = \Delta \varphi (1 + 6u) - \frac{1}{4} \Delta^2 \varphi + \dots.$$

Estimating $u = 0.25$, gives a translational velocity

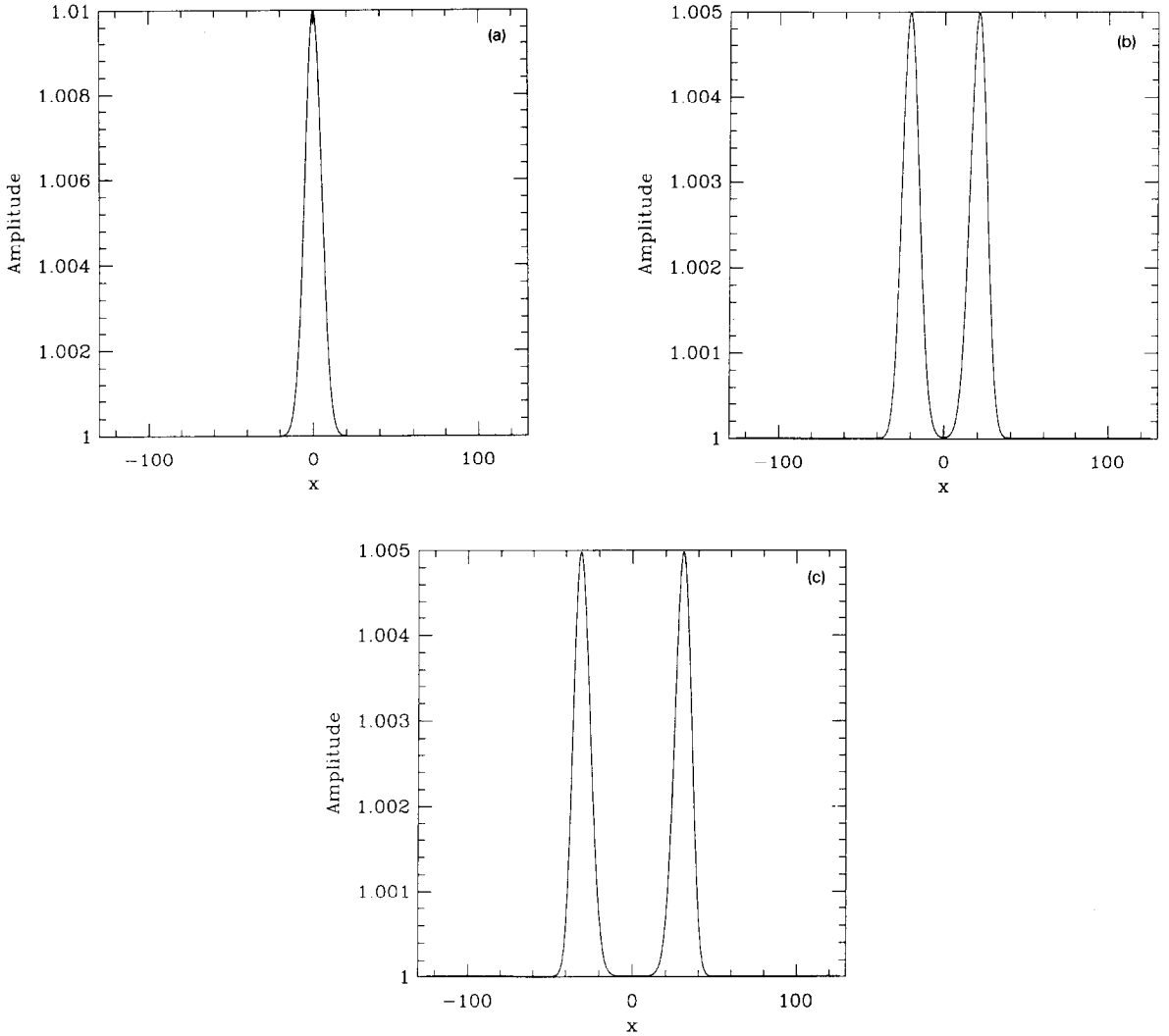


Fig. 1. Numerical integration of NLSE with an initial perturbation of small amplitude ($a = 0.01$) and large width ($l = 10\xi$): (a) amplitude of the initial data, (b) amplitude of the solution at $t = 20$, (c) amplitude of the solution at $t = 30$.

$\|\mathbf{v}\| = 1.58$ that is in agreement with the measured one within 5%. We found that dispersion is noticeable for $l \lesssim 5\xi$ and that nonlinearity sets in for $a \gtrsim 0.3$.

3. Numerical study of a system of vortices in the NLSE

It has been known for some time that the equations of motion for a dilute gas of vortices

described by NLSE are similar to the ones of inviscid incompressible fluid dynamics [6–8]. This similarity can be understood by scaling space and time as $|\nabla| = \epsilon$ and $\partial/\partial t = \epsilon^2$ and expanding the variables in the form:

$$\rho = \rho_0 + \epsilon\rho_1 + \epsilon^2\rho_2 + \dots, \quad (18)$$

$$\mathbf{v} = \epsilon\mathbf{v}_1 + \epsilon^2\mathbf{v}_2 + \dots. \quad (19)$$

We get from equations (3) and (4)

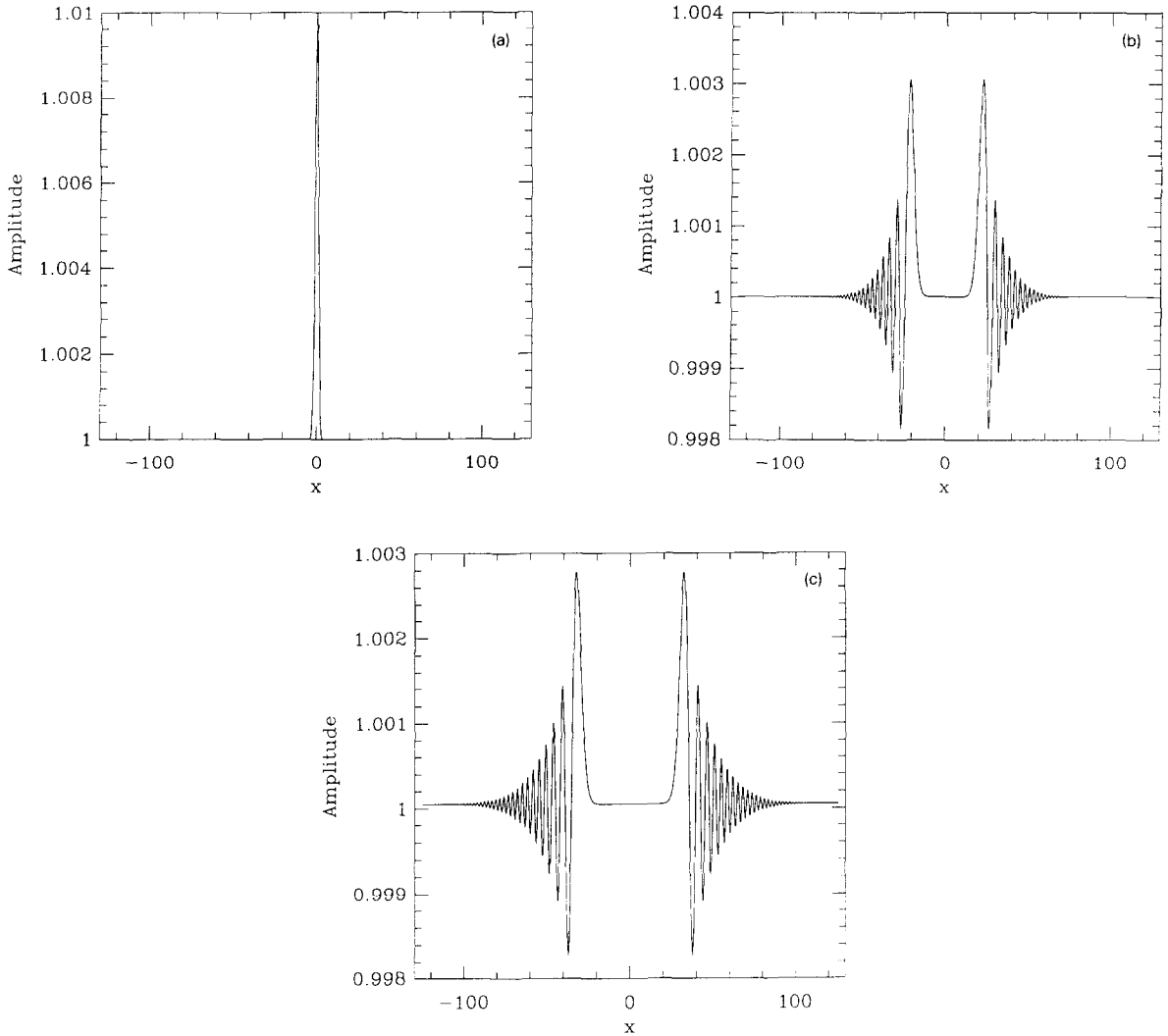


Fig. 2. Same as fig. 1 but $l = 2\xi$. Note that dispersive effects are now visible on the solution.

$$\nabla \cdot \mathbf{v}_1 = 0, \quad (20)$$

$$\frac{\partial \mathbf{v}_1}{\partial t} + (\mathbf{v}_1 \cdot \nabla) \mathbf{v}_1 = -\nabla \rho_2, \quad (21)$$

with $\rho_0 = 1$ and $\rho_1 = 0$. The velocity field far from the vortices thus obeys the incompressible Euler equation. It can then be argued that the dominant effect of far-away vortices on one vortex results in a Galilean boost with a global velocity that is the sum of the velocities induced by each

of the far-away vortices [6]. However this type of argument neglects compressible effects. Indeed it was recently claimed that acoustics modifies the dynamics of two counter rotating vortices [9].

In order to investigate numerically these delicate problems, we chose to work with a Fourier pseudo-spectral method both for its precision and its ease of implementation. We used the same scheme as the one described in section 2 extended to two space dimensions. To study the motion of vortices in NLSE with periodic bound-

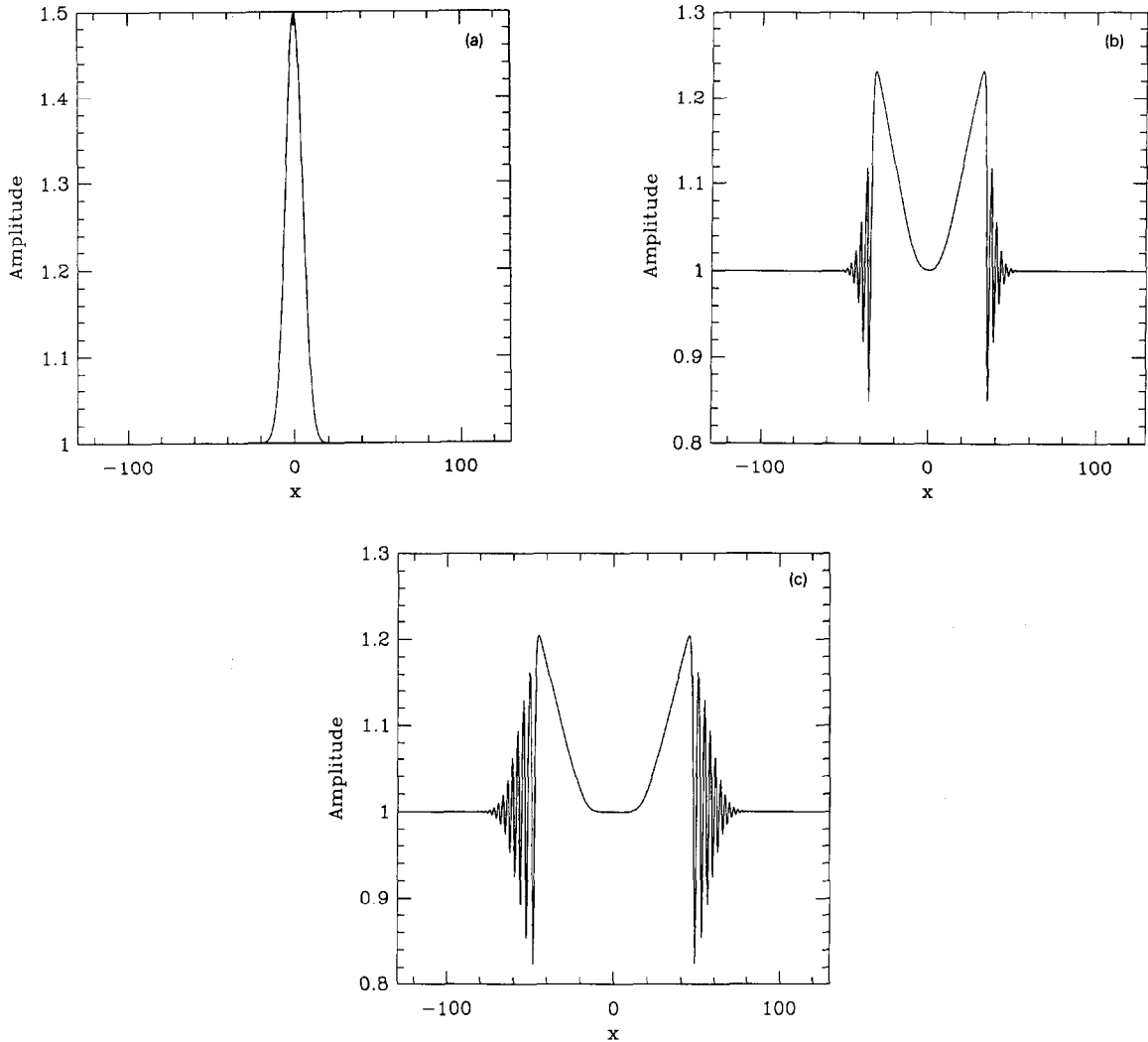


Fig. 3. Same as fig. 1 but $a = 0.5$. Note that scales significantly smaller than the length scale on the initial data have been generated through nonlinear effects.

any conditions, we need to start from an initial field that minimizes the acoustic emission. We have found convenient to prepare it using the real Ginzburg–Landau equation (RGLE):

$$\frac{\partial A}{\partial t} = A + \frac{1}{2} \Delta A - |A|^2 A. \quad (22)$$

Indeed the solution of this equation can be shown to converge rapidly toward a time independent solution of NLSE both in the case of

a vortex free condensate and in the case of one isolated vortex. It is well known that following RGLE dynamics, vortices of opposite sign move toward each other and eventually collapse [10].

Our procedure to prepare the initial data is as follows: we first initialize a periodic complex field with a system of zeros at given spatial localizations. We then let the field evolve through RGLE dynamics on a time scale sufficient for amplitude relaxation. Eventually RGLE dynamics will lead to vortex–antivortex

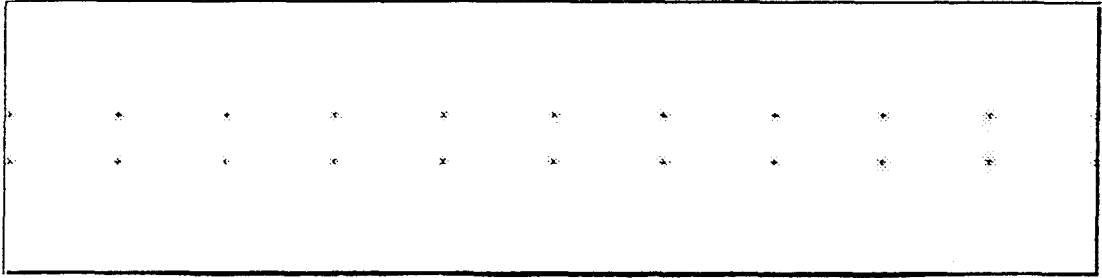


Fig. 4. Initial data corresponding to a periodic array of ten counter rotating vortices. The amplitude of the field is displayed in this raster visualization, small amplitude regions (i.e. the core of the vortices) appear in dark.

annihilation but we terminate it before this happens. The field obtained with this procedure is then used as initial data for NLSE dynamics. After a short transient when the system adapts to NLSE dynamics by generating some small acoustic perturbations, we observe an Eulerian behavior for the system of vortices. Our two numerical codes for the integration of 2D RGLE and 2D NLSE have been tested respectively against previously published results for defect-antidefect interaction [10] and against our 1D results for NLSE, by using x -constant or y -constant initial data. The results presented below

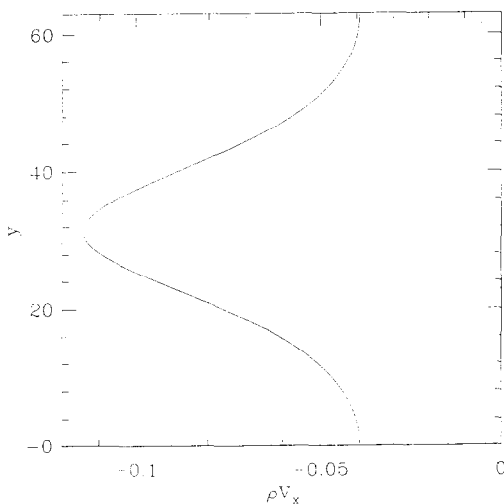


Fig. 5. A plot of the mass flux ρv_x as a function of y , midway between pairs of counter rotating vortices. Note that with our choice of initial data, the jet is flowing to the left.

needed 400×100 Fourier modes to achieve spectral convergence.

To check the possibility of reproducing numerically the Eulerian dynamics of point vortices in NLSE, we chose as a test problem to study the destabilization of an array of counter rotating vortices. This system is a classical discrete model of a 2D jet and has been thoroughly studied [11]. It is known to lose stability for two families of perturbations, the so-called sinuous and varicose modes. We prepared with our “RGLE method” a jet formed by ten periodically disposed counter rotating vortices. The distance between two successive pairs is $a = 42.7\xi$, each pair is separated by $b = 18.2\xi$. The computational box has periodicity lengths $L_x = 10a$ and $L_y = 5.9b$. These initial data are visualized in fig. 4 and the corresponding mass flux is shown in fig. 5. Using this field as initial data for NLSE resulted in a uniform motion of the vortex array up to $t = 800$ without noticeable destabilizations. We have measured the velocity of the vortex array ($v = 0.12$), it agrees with that of Eulerian point vortices within 2%. In order to minimize computer time, we imposed initial perturbations by slightly translating the vortices with a variable periodic field corresponding to the modes of the linear theory [11]. Fig. 6 displays the evolution for a sinuous initial perturbation and fig. 7 for a varicose initial perturbation. The vortex system is seen to evolve as predicted and the acoustic background remains weak.

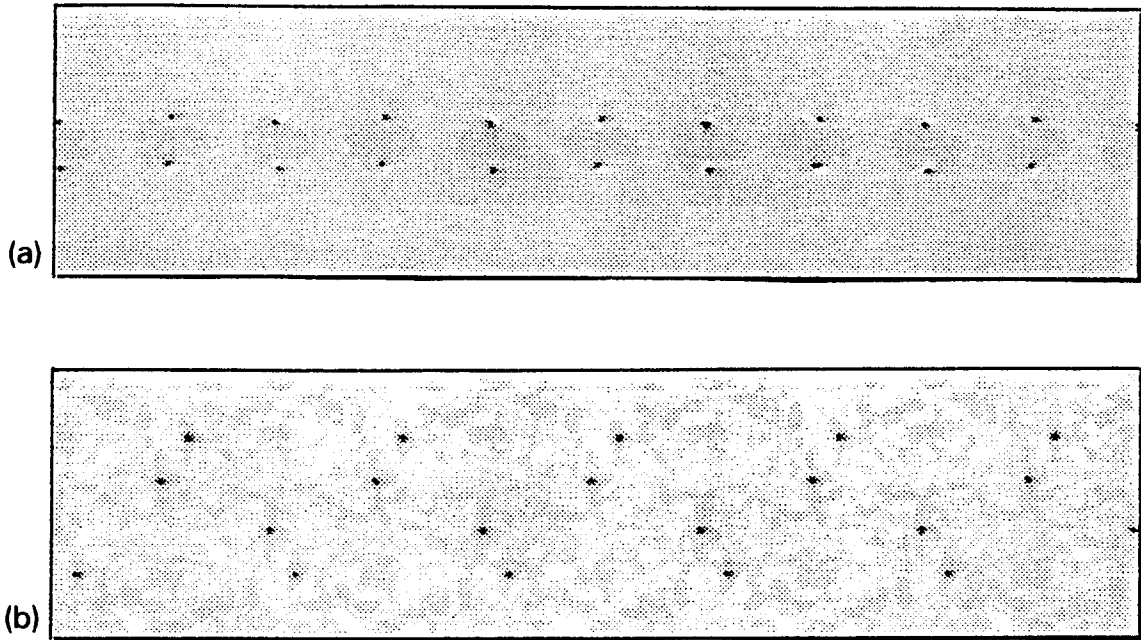


Fig. 6. Sinuous destabilization of the jet: (a) raster visualization of the slightly perturbed initial data; (b) result of NLSE evolution at $t = 550$.

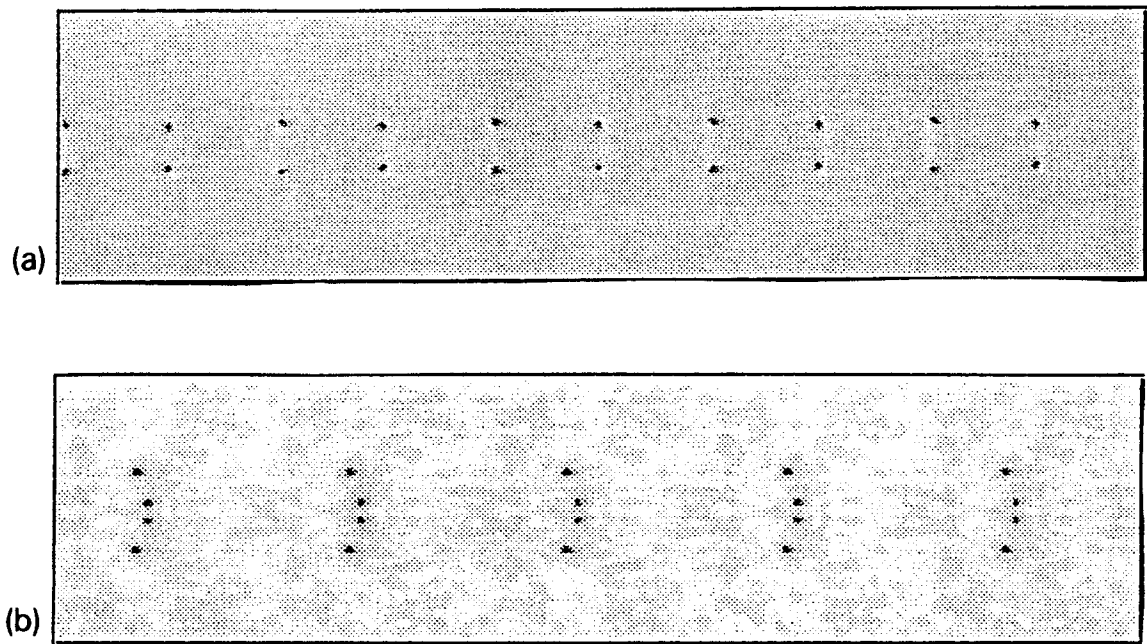


Fig. 7. Same as fig. 6 but for a varicose destabilization ($t = 400$).

4. Conclusion

In summary, our results obtained through asymptotic expansions and direct numerical simulations point to the feasibility of obtaining genuine hydrodynamical behavior in NLSE. We were able to get separately from NLSE nonlinear and dispersive acoustics and Eulerian dynamics of point vortices. In order to get a definite answer for the delicate and non trivial problem of vortex-sound interactions and emission of sound by vortices, the choice of numerical method is crucial. We have checked that the simple Fourier pseudo-spectral method we have used was spectrally converging in the cases studied in this paper, it therefore ensured a degree of precision unmatched by finite difference methods. However our method requires to work with periodic data. This is clearly a disadvantage when studying sound emission: this necessitates a periodicity length greater than the distance travelled by the emitted sound. In this context, finite difference methods allow for absorbing boundaries and may then be the right choice [9]. Another possibility worth noticing is to use spatially unbounded spectral expansions, such as mapped Chebyshev polynomials.

References

- [1] A.C. Newell, *Solitons in Mathematics and Physics*, Soc. Ind. Appl. Math. (1985).
- [2] H. Ono, Nonlinear wave modulation in inhomogeneous media, *J. Phys. Soc. Japan* 37 (1974) 1668–1672.
- [3] R.J. Donnelly, *Quantized Vortices in Helium II* (Cambridge Univ. Press, Cambridge, 1991).
- [4] E.A. Spiegel, Fluid Dynamical Form of the Linear and Nonlinear Schrödinger Equations, *Physica D* 1 (1980) 236–240.
- [5] D. Gottlieb, S.A. Orszag, *Numerical Analysis of Spectral Methods: Theory and Applications*, Soc. Ind. Appl. Math., Philadelphia (1977).
- [6] A.L. Fetter, Vortices in an imperfect Bose gas IV. Translational Velocity, *Phys. Rev.* 151 (1966) 100–104.
- [7] F. Lund, Defect Dynamics for the Nonlinear Schrödinger Equation Derived from a Variational Principle, *Phys. Lett. A* 159 (1991) 245–251.
- [8] J.C. Neu, Vortices in complex scalar fields, *Physica D* 43 (1990) 385–406.
- [9] T. Frisch, Y. Pomeau and S. Rica, Transition to dissipation in a model of superflow, *Phys. Rev. Lett.* 69 (1992) 1644–1647.
- [10] E. Bodenschatz, A. Weber and L. Kramer, Interaction and Dynamics of Defects in Convective Roll Patterns of Anisotropic Fluids, *J. Stat. Phys.* 64 (1991) 1007–1015.
- [11] H. Lamb, *Hydrodynamics* (Cambridge Univ. Press, Cambridge, 1932).